

15C.4 Downdrafts and the Evolution of Boundary Layer Thermodynamics in Hurricane Earl (2010) Before and During Rapid Intensification

Joshua B. Wadler^{1*}, Jun A. Zhang^{2,3}, Benjamin Jaimes¹, Lynn K. Shay¹

¹Rosenstiel School of Marine and Atmospheric Science, University of Miami, Miami, FL

²NOAA/Atlantic Oceanographic and Meteorological Laboratory/Hurricane Research Division

³Cooperative Institute for Marine and Atmospheric Studies, University of Miami, Miami, Florida

1. Introduction

Tropical Cyclone (TC) Earl (2010) was a heavily sampled storm in the western Atlantic basin that formed on 25 August 2010 and dissipated on 5 September 2010. While there are many studies on why Earl underwent rapid intensification (RI; greater than 30 knot increase in intensity over 24 hours), this study focuses on the role of downdrafts in Earl's intensity evolution.

Downdrafts are generally thought to negatively impact TC intensity since they can transport low equivalent potential temperature (θ_e ; also referred to as moist entropy) air into the boundary layer. Two types of downdrafts are identified in this study: those catalyzed by evaporation of a precipitation core (e.g. Riemer et al. 2010; Tang and Emanuel 2010, 2012; Molinari et al. 2013), and those catalyzed from upper-level convergence associated with vortex tilt (e.g. Reasor et al. 2013; DeHart et al. 2014).

There are two leading scenarios for which downdraft-induced low θ_e air impacts TC intensity. First, if low θ_e air is advected into the eyewall, it reduces the amount of work that is done through the Carnot cycle (Emanuel 1986; Tang and Emanuel 2010;

Riemer et al. 2010). Second, if low θ_e air is advected around the storm into the downshear-right (DSR) quadrant, it inhibits the development of new convection (Zhang et al. 2013; Zhang et al. 2017).

This study describes the evolution of boundary layer thermodynamics in Hurricane Earl before and during RI. Specifically, we examine how different types of downdrafts influence the boundary layer thermal structure and how Earl overcame the negative impact of downdrafts on its intensification.

2. Data and Methodology

Periods right before intensification (P1) and during intensification (P2) are analyzed in this study. We utilize tail Doppler radar analyses from the NOAA WP-3D aircraft from flights on 28 August 2010 (P1) and 29 August 2010 (P2). Additionally, we utilize dropsonde data from NOAA and NASA aircraft. The thermodynamic data from the dropsondes was interpolated to a horizontal grid at 10-m. At each dropsonde splash location, radial cross sections through the overlaid radar data were taken. Locations with significant vertical velocities ($> 0.5 \text{ m s}^{-1}$) are called Dropsonde Points of Interest (DPoIs). The goal is to investigate the source

of the thermodynamic signatures seen in the dropsondes. This type of analysis assumes that the thermodynamic features observed in the dropsondes are caused by dynamic features in the radar analyses. Lastly, to calculate air-sea enthalpy (latent heat plus sensible heat) fluxes, we utilize satellite and drifter-based sea-surface temperature data interpolated to the dropsonde splash locations and presented in Jaimes et al. (2015).

3. Results and Discussion

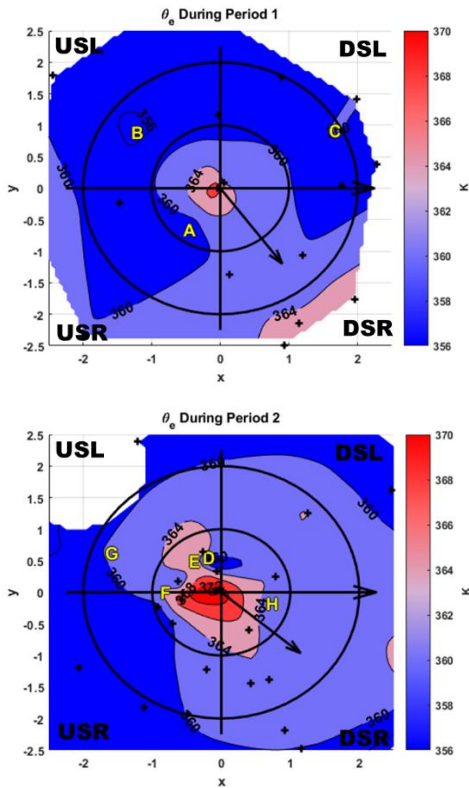


Figure 1: Normalized radial and shear-rotated (pointing to the right) 10-m air 10-m θ_e during (a) P1 and (b) P2. Storm motion is indicated by the short black arrow, and radial bands of $r^* = 1$ and $r^* = 2$ are overlaid. DpoIs are in letters and '+' represent other dropsonde splash locations.

The 10-m θ_e during the two periods is shown in Figure 1. During both periods, there is thermodynamic variability both inside the RMW and in the outer-core. To further

explore the sources of the low and high θ_e signatures inside the radius of maximum winds, two DPoIs are analyzed in the upshear-left quadrant, a location where convective characteristics are strongly linked to hurricane intensity change (e.g. Rogers et al. 2013; Wadler et al. 2018).

Vertical profiles of the dropsondes through DPoI A (low θ_e) and DPoI E (high θ_e) are compared to the mean sounding during their respective time periods (Figure 2). In both cases, the θ_e signatures reflected at 10-m are related to physical processes in upper part of the boundary layer (determined as height with 10 percent of the peak inflow following Zhang et al. 2011).

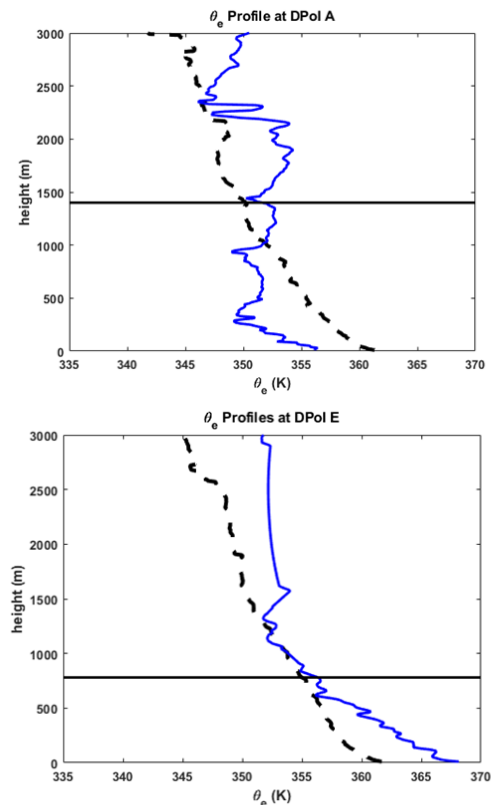


Figure 2: Quasi-vertical profiles of θ_e from the dropsondes at (a) DPoI A and (b) DPoI E. The average boundary layer height for each period is shown in the thick dashed line. The dashed line represents the mean sounding during each period.

The variability in the θ_e field with height largely resembles variability in specific humidity (Figure 3) rather than temperature (not shown). Thus, the change in inner-core θ_e can be attributed to changes in the moisture fields. To explore what can cause the specific humidity anomalies, cross sections through the overlaid tail Doppler radar data are examined (Figure 4).

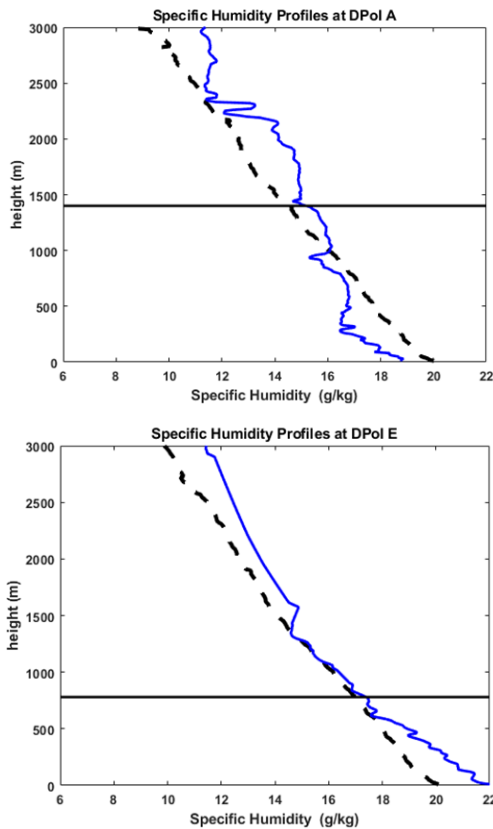


Figure 3: As in Figure 2, but for specific humidity.

DPOI A, the point with low surface θ_e , has a cross section characterized by a weak ($< 2 \text{ m s}^{-1}$) near-surface downdraft. The presence of substantial hydrometeors and weak vertical motions, along with the low specific humidity values, indicate that little evaporation took place at this location. This

thermodynamic signature is consistent with cool air outflow from updrafts that cannot adiabatically warm because of weak vertical velocities. On the contrary, the cross section through DPOI E shows a downdraft exceeding 2 m s^{-1} maximized at $\sim 4 \text{ km}$ altitude. The large vertical velocities could stem from large evaporation rates in the precipitation core creating negative buoyancy. The evaporation leads to the large specific humidity values that the dropsonde interacted with and control the high θ_e observed at 10-m.

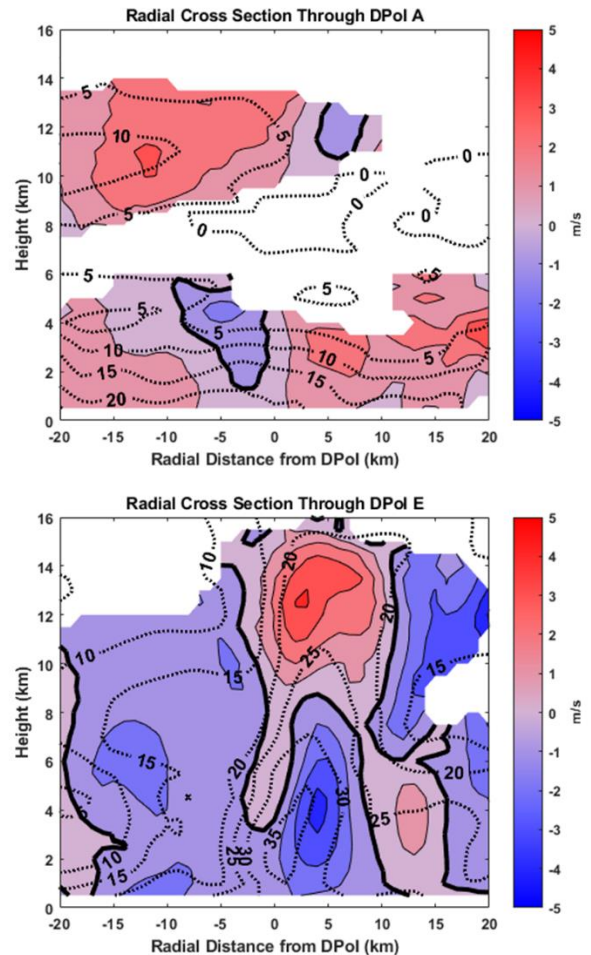


Figure 4: Radial cross-sections through Doppler radar data from the WP-3D aircraft for (a) DPOI A and (b) DPOI E. Shading is vertical velocity with the zero contour in thick black. Dashed lines are reflectivity.

The potential for boundary layer recovery was also examined. Since Earl underwent rapid intensification, it is likely that the boundary layer recovered from the negative impacts of downdrafts. Potential recovery mechanisms include air-sea enthalpy fluxes, atmospheric turbulent eddies/mixing, eye-eyewall mixing, and heat fluxes from above.

4. Summary and Conclusions

Differences in inner-core surface θ_e observed by dropsondes during Hurricane Earl was attributed to differences in specific humidity in the boundary layer and types of downdrafts encountered. The dropsonde with lower 10-m θ_e likely interacted with a weak ($< 2 \text{ m s}^{-1}$) downdraft that has low evaporation rates. The dropsonde with higher 10-m θ_e likely interacted with a strong downdraft that has high evaporation rates. Overall, this makes the weaker inner-core downdraft more detrimental to storm intensification. Since Earl began intensifying after P1 and continued intensifying during P2, it is likely that the boundary layer recovered quickly from the low θ_e intrusions through air-sea enthalpy flux.

5. Acknowledgements

We thank the people of the NOAA Aircraft Operations Center who helped to collect this data. The work is funded through the NSF Graduate Research Fellowship.

6. References

DeHart, J. C., R. A. Houze, and R. F. Rogers, 2014: Quadrant distribution of tropical cyclone inner-core kinematics in relation to environmental shear. *J. Atmos. Sci.*, **71**, 2713–2732.

Jaimes, B., L.K. Shay, and E.W. Uhlhorn, 2015: Enthalpy and Momentum Fluxes during Hurricane Earl Relative to Underlying Ocean Features. *Mon. Wea. Rev.*, **143**, 111–131.

Molinari, J., J. Frank, and D. Vollaro, 2013: Convective Bursts, Downdraft Cooling, and Boundary Layer Recovery in a Sheared Tropical Storm. *Mon. Wea. Rev.*, **141**, 1048–1060, doi: 10.1175/MWR-D-12-00135.1.

Reasor, P. D., R. F. Rogers, and S. Lorsolo, 2013: Environmental flow impacts on tropical cyclone structure diagnosed from airborne Doppler radar composites. *Mon. Wea. Rev.*, **141**, 2949–2969.

Riemer, M., M. T. Montgomery, and M. E. Nicholls, 2010: A new paradigm for intensity Modification of tropical cyclones: Thermodynamic impact of vertical wind shear on the inflow layer. *Atmos. Chem. Phys.*, **10**, 3163–3188.

Rogers, R. F., P. D. Reasor, and S. Lorsolo, 2013a: Airborne Doppler observations of the inner-core structural differences between intensifying and steady-state tropical cyclones. *Mon. Wea. Rev.*, **141**, 2970–2991.

Tang, B., and K. Emanuel, 2010: Midlevel ventilation's constraint on tropical cyclone intensity. *J. Atmos. Sci.*, **67**, 1817–1830.

Tang, B., and K. Emanuel, 2012: Sensitivity of tropical cyclone intensity to ventilation in an axisymmetric model. *J. Atmos. Sci.*, **69**, 2394–2413.

Wadler, J.B., R.F. Rogers, and P.D. Reasor, 2018: The Relationship Between Spatial Variations in the Structure of Convective Bursts and Tropical Cyclone Intensification as Determined by Airborne Doppler Radar. *Mon. Wea. Rev.*, **146**, 761–780.

Zhang, J.A., R.F. Rogers, D.S. Nolan, and F.D. Marks, 2011: On the Characteristic Height Scales of the Hurricane Boundary Layer. *Mon. Wea. Rev.*, **139**, 2523–2535.

Zhang, J., R. Rogers, P. Reasor, E. Uhlhorn, and F. Marks, 2013: Asymmetric Hurricane Boundary Layer Structure from Dropsonde Composites in Relation to

the Environmental Vertical Wind Shear. *Mon. Wea. Rev.*, **141**, 3968–3984.

Zhang, J.A., J.J. Cione, E.A. Kalina, E.W. Uhlhorn, T. Hock, and J.A. Smith, 2017: Observations of infrared sea surface temperature and air-sea interaction in Hurricane Edouard (2014) using GPS dropsondes. *J. Atmos. Oceanic Technol.*, **34**, 1333-1349.